

Microstructure, Properties and Atomic Level Strain in Severely Deformed Rare Metal Niobium

Lembit KOMMEL^{1*}, Mart SAARNA¹, Rainer TRAKSMAA², Igor KOMMEL³

¹Department of Materials Engineering, Ehitajate tee 5, 19086 Tallinn, Estonia

²Materials Research Center, Tallinn University of Technology, Ehitajate tee 5, 19086 Tallinn, Estonia

³All Russian Institute of Standards, Str. Ozernaja 46, 119361 Moscow, Russia

crossref <http://dx.doi.org/10.5755/j01.ms.18.4.3091>

Received 29 August 2011; accepted 18 September 2011

The mechanical and physical properties relationship from atomic level strain/stress causes dislocation density and electrical conductivity relationship, as well as crystallites deformation and hkl-parameter change in the severely deformed pure refractory rare metal Nb at ambient temperature and during short processing times. The above mentioned issues are discussed in this study.

For ultrafine-grained and nanocrystalline microstructure forming in metal the equal-channel angular pressing and hard cyclic viscoplastic deformation were used. The flat deformation and heat treatment at different parameters were conducted as follows. The focused ion beam method was used for micrometric measures samples manufactured under nanocrystalline microstructure study by transmission electron microscope. The microstructure features of metal were studied under different orientations by X-ray diffraction scattering method, and according to the atomic level strains, dislocation density, hkl-parameters and crystallite sizes were calculated by different computation methods.

According to results the evolutions of atomic level strains/stresses, induced by processing features have great influence on the microstructure and advanced properties forming in pure Nb. Due to cumulative strain increase the tensile stress and hardness were increased significantly. In this case the dislocation density of Nb varies from $5.0E+10 \text{ cm}^{-2}$ to $2.0E+11 \text{ cm}^{-2}$. The samples from Nb at maximal atomic level strain in the (110) and (211) directions have the maximal values of hkl-parameters, highest tensile strength and hardness but minimal electrical conductivity. The crystallite size was minimal and relative atomic level strain maximal in (211) orientation of crystal. Next, flat deformation and heat treatment increase the atomic level parameters of severely deformed metal.

Keywords: rare metal, severe plastic deformation, microstrains, dislocation density.

INTRODUCTION

The processing of bulk metallic materials using severe plastic deformation (SPD) techniques [1, 2] has recently become of importance in many research laboratories around the world. Using these methods [3] enable to change the metals' microstructure on ultrafine-grained (UFG) or even on nanocrystalline (NC) level. The severely deformed ultrafine-grained (UFG) refractory rare metals niobium (Nb) and tantalum (Ta) have drawn attention in many areas of advanced industries due to their unique properties such as combination of high temperature melting point and service, chemical resistance as well as high-strength and good ductility [4–8]. Thus, the fine-grained Nb is used as mint metal [9] and in composite Nb3Sn superconductors' applications as a precursor fine filament within a pure copper (Cu) matrix [10]. The fabrication of UFG ($100 \text{ nm} < \text{grain size (GS)} < 1000 \text{ nm}$) and nanostructured (NS) ($\text{GS or crystallite size (CS)} < 100 \text{ nm}$) pure metals, alloys and composites using severe plastic deformation (SPD) techniques evolved rapidly advancing direction of modern nano-materials science in the last decade. Among the many techniques available for producing nanostructured materials, the equal-channel angular pressing (ECAP) is the most popular and rapidly developing one.

These techniques aimed to develop advanced ultra-strength materials with improved mechanical, physical, chemical, tribological, etc. properties [11, 12] for application in aircraft, automobile, medical, electronic etc. industries [13]. Therefore, SPD techniques have proved to be the most efficient and low cost methods used in industry as compared to other well known methods of nanotechnology. In the latest investigation of nanocrystalline metals physical properties were established [14] proving that commercially pure copper (Cu) with high angle grain boundaries (HAGBs) microstructure and lowered by hard cyclic viscoplastic (HCV) deformation [15, 16] dislocation density has increased electrical conductivity properties. Consequently, the dislocation density increases electrical resistance like alloying elements and impurities in alloys in comparison with pure metals. It was found [17] that NC Cu after HCV deformation and after low temperature heat treatment with very low ($1-2 \text{ }^\circ\text{C}/\text{min.}$) heating rate in vacuum up to $200 \text{ }^\circ\text{C}$ shows true stress at tension up to 1500 MPa , which is about 30 times higher as compared to some annealed Cu used.

Two principal factors cause the properties of nanomaterials to differ significantly from other conventional materials. They have increased relative surface area of nanograins (nanoparticles) per mass as a particle decreases in size, a greater proportion of atoms are found on the surface as compared to those inside [18]. Thus, nanoparticles have a much greater surface area per unit mass as compared to large particles. These factors can

*Corresponding author. Tel.: +372-620-3356; fax.: +372-620-3196.
E-mail address: lembit.kommel@ttu.ee (L. Kommel)

change or enhance properties of nanometals such as chemical reactivity (corrosion behavior) [19], irradiation behavior [20], as well as superior tension strength, hardness, superplasticity, low temperature ductility, electrical conductivity, high temperature superconductivity, etc. The latest investigations [21–27] demonstrate the microstructure and mechanical-physical properties relationship from atomic level strains/stresses, also causes phase transformations as well as dislocation density change in the material at ambient temperature and during short processing times. The evolutions of physical and mechanical properties as well as their microstructures of different metals during SPD processing's depend on changes in their atomic structure [21], atomic level stresses [22], atomic level strains (relative microstrains) [23], atomic level behavior of crystals defects [24, 25], etc. For the determination of micromechanical fields on atomic scale and characterization [26] in plastically and severely deformed nanocrystalline materials the fast Fourier transform-based modeling [27] at latest years can be used. The aim of this study is to provide a platform product for pure refractory rare metal Nb microstructure and properties changes during SPD processing's and these changes dependence on atomic level strain.

MATERIALS AND METHODOLOGY

In the current study we used commercially pure Nb produced from Molycorp Silmet AS, Estonia, well known as world-wide rare metals and rare earth metals producer. According to quality certificate the Nb was of 99.95 wt. % purity. The metals used in the present study were double electron beam melted (DEBM) cast ingot with ~218 mm in diameter and ~2.5 m in length. The Nb ingots have an as-cast microstructure with measured grains up to 2 cm–4 cm in diameter and 20 cm–40 cm in length. Such grains distributions in ingots were determined by hardnessmeter BRIN 200 with measurement capability of $\pm 2\%$ according to EVS EN ISO 6506-1 standard. The hardness of Nb varies from 77HB30 to 122HB30, respectively. For processing by ECAP the bars with nominal dimensions of (14×14×150) mm were cut off from ingots with their long axes parallel to the ingot axis. Before SPD the specimens were preliminarily subjected to heat treatment in vacuum furnace at temperature of 1100 °C for 2 h. To decrease friction and eliminate the cold adhesion at friction welding of Nb to walls of ECAP die channels the bars were covered with copper film and lubricated with copper-graphite-oil slush. For processing of UFG microstructure in the hard to deformation Nb samples we used ECAP die of new construction [28]. The punch has a channel for sample and the straining process at lowered friction is similar to that of the conventional ECAP. The 12 passes of ECAP by B_c route were conducted and the calculated maximal collected von Mises strain of ~13.8 was received. From the ECAP processed samples test samples were manufactured for HCV deformation testing (Fig. 1). The HCV deformation [15] of ECAP processed samples was conducted by means of materials testing installation Instron-8516. Cycling was conducted with frequency of 0.5 Hz for all strain levels. By strain amplitude increase the strain rate was increased, respectively.

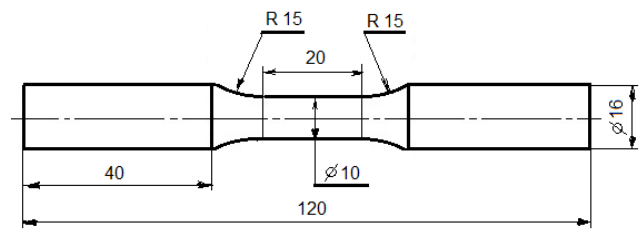


Fig. 1. Schematic illustration of the test sample for HCV deformation. The true strain was measured by extensometer with base of 20 mm in length on cross-section of 10 mm in diameter

The viscoplastic straining was conducted at tension-compression strain amplitudes of ± 0.1 , ± 0.2 , ± 0.5 , ± 1 and $\pm 1.5\%$ for 20 cycles, respectively. The ECAP processed samples Young module at tension of 0.1 % and 0.2 % was measured at load increase with 1 MPa/s before and after HCV deformation. It is well known, that SPD processed UFG metals for use in different constructions need future deformation or cutting via conventional metal working methods. Therefore, from different ECAP processed as well from HCV deformed specimens (see Fig. 1) with ~10 mm in length samples were cut off and then flat die forged in longitudinal and cross-section directions to 3 mm in thickness, so that the test area has a diameter of 20 mm or over. Such samples and samples with no flat die forged for X-ray diffraction investigations, indentation testing and electrical conduction measure were used. The hardness was measured by Mikromet 2001 with load of 0.2 kg for 12 s and by Zwick Z2.5/TS1S at load of 50 N according to EVS-EN ISO14577-1-2003 standard. For TEM templates manufacturing we used focused ion beam (FIB) (FEI Company Helios NanoLab.) instrument. The micro templates with measures of (5×10) μm and thickness of 40 nm were cut off in longitudinal and transverse directions to sample axis. Using in situ transmission electron microscopy (TEM, EMV-100BR) method we studied the microstructure of metals in these directions. The X-ray diffraction (XRD) using Cu-K α radiation for qualitative and quantitative analyses of microstructure the Bruker X-ray diffractometer D5005 was used. The X-ray diffraction investigation was conducted from 30° to 142° of 2-Theta Scale. The 8 XRD-reflections for heat treated raw structure and SPD processed nanocrystalline structure at different testing planes like transverse plain (TP), normal plane (NP) and cross-section plane (CS) of samples were received. The parameters of reflections (110), (200) and (211) were chosen for calculations of crystallite size and atomic level strain [29]. The dislocation density and distribution of dislocation [30] was calculated on parallel atomic lattices of (110) (220) and (200) (400), respectively. For study the atomic level strain (with compare to etalon of LaB $_6$) and crystallite size the Lorenz [29] and for dislocation densities study the Reehinger, Williamson-Hall and Warren-Averbach [30] computation methods were used. The properties were calculated according to (110), (200) and (211) directions and in parallel plains of (110)–(220) and (200)–(400) of crystallites, respectively. The electrical conductivity in megasiemens per meter (MS/m) was determined with the measurement uncertainty of $\pm 1\%$ for different interatomic

stress levels and orientations by means of Sigmatest 2.069 (Foerster) according to NPL (National Physical Laboratory, England) standards at 60, 120 and 480 kHz on calibrated area of 15 mm in diameter.

RESULTS AND DISCUSSIONS

During SPD processing by ECAP at 12 passes by B_c route the Martens hardness of pure Nb was increased from $HM_{50/8/16} = 640 \text{ N/mm}^2$ to $HM_{50/8/16} = 1930 \text{ N/mm}^2$ (correlation to Vickers hardness is 60–181HV5) (Fig. 2, a). The Martens hardness was slightly higher in transverse plane (TP) than in cross-section (CS) of ECAP processed specimen. During HCV deformation at 5 test series the Martens hardness of Nb (Fig. 2, b) was increased from $HM_{50/8/16} = 620 \text{ N/mm}^2$ to $HM_{50/8/16} = 1300 \text{ N/mm}^2$ (correlation to Vickers hardness is 57–122 HV5) and creep decreased from 6.1 to 4.7 in the middle part of tension-compression test specimen (see Fig. 1). During processing the yield strength of Nb was increased about four times and material has good ductility properties as the elastic reformation work was increased [22, 23]. By this the relation of elastic work to total work of indentation was increased about two times. The microhardness was step-by-step increased and creep decreased during each pass of ECAP, respectively.

The hardness parameters of Nb decrease during cold flat deformation and increase during low temperature heat treatment at 170°C and show maximal values after heat treatment at 350°C as a result of atomic structure correlation on grain boundaries [8].

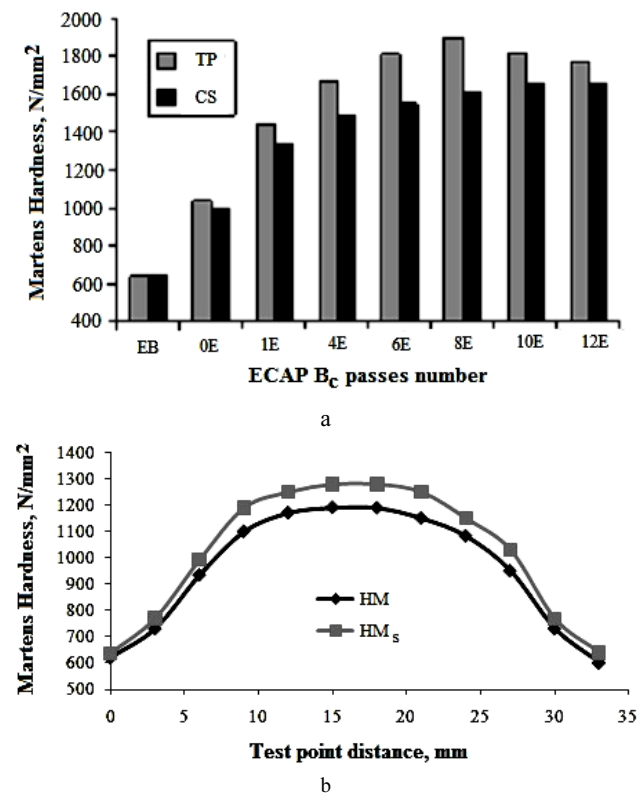


Fig. 2. Influence of ECAP processing's (a) and HCV deformation (b, in TP) on Martens hardness of pure Nb

Also the results of present investigation show that during HCV deformation the Young's modulus (Fig. 3) and yield strength were decreased for samples with 6–12

ECAP passes by B_c route with UFG microstructure while samples with coarse grained (CG) or fine grained (FG) microstructures shows strain hardening behavior at HCV deformation [5].

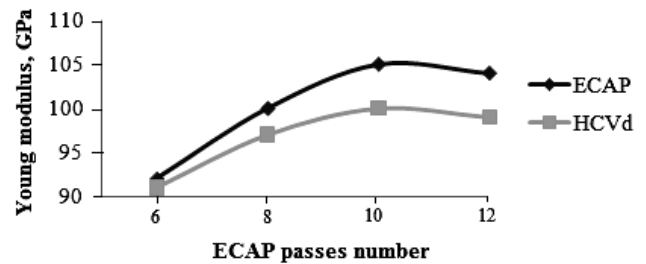


Fig. 3. ECAP and followed HCV deformation influence on Young module evolution of pure Nb

During SPD processing, dependence on cumulative strain increases the crystallite size was decreased to nanometric scale (Fig. 4, a) and material took homogenized but the mechanical properties (see Fig. 2, a) as well microstructure in the TP, NP and CS planes are different. The nanocrystalline microstructure in Nb with mean grain sizes below 100 nm was received in cross-section of ECAP sample. At increased cycle's number of HCV deformation the nanograins coalescence starts (Fig. 4, b).

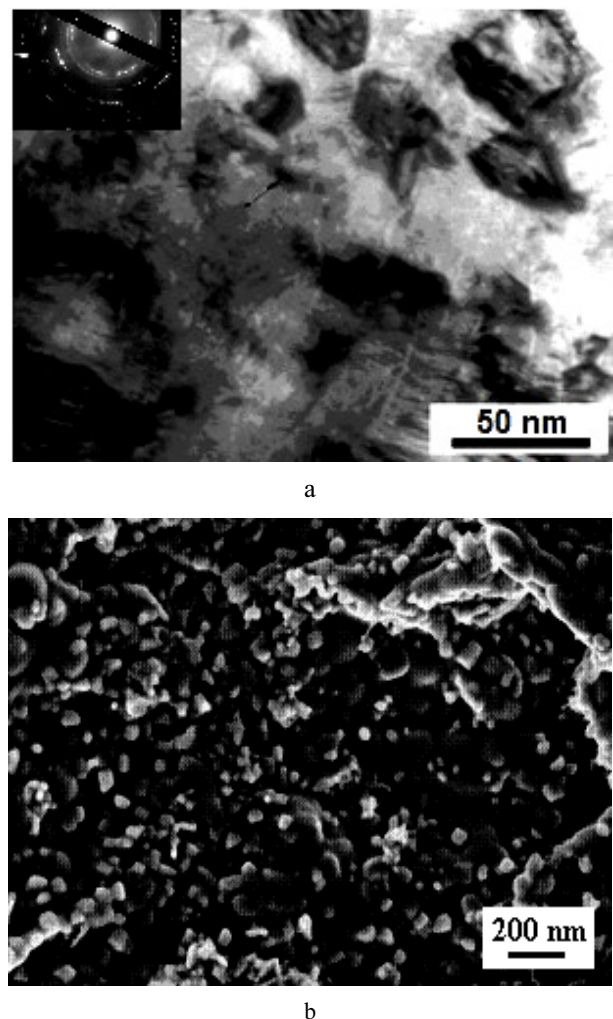


Fig. 4. TEM picture of microstructure of (ECAP) sample (a) and FE SEM picture of the fractured surface (b) of tension sample after ECAP and followed HCV deformation

The TEM (Fig. 4, a) and FE SEM (Fig. 4, b) pictures presents that microstructure of pure Nb received by ECAP and microstructure of fractured surface (followed HCV deformation and tension straining) are both NC. The fracture mechanism, mechanical and physical properties of SPD processed Nb differs as compared to samples with conventional CG microstructure and need future investigation.

The seven X-ray reflections of pure Nb for different atomic planes of crystallite orientations in Fig. 5 are presented. For the investigated peaks under consideration the XRD reflections intensities were minimal for electron beam melted (EB), as cast and heat treated metal (S1-EB-TP) and the intensities were increased by cumulative strain increase during SPD processing (Fig. 6).

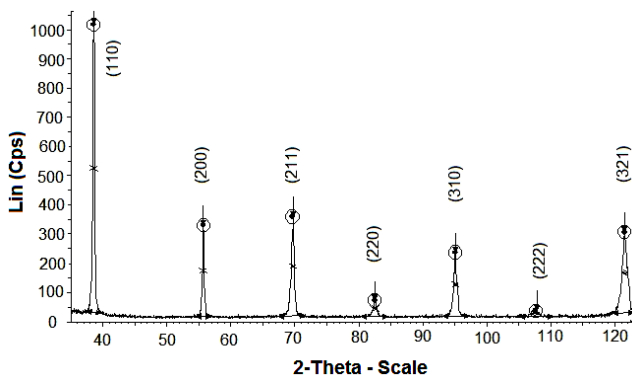


Fig. 5. X-ray diffraction patterns of pure Nb for atomic level micromechanical properties study

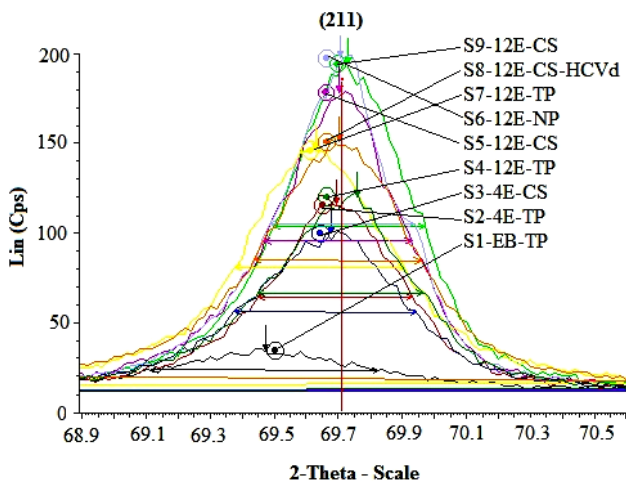


Fig. 6. X-ray reflections in crystallite plane of (211) (with different intensities) for study of atomic level strain and micromechanical properties of samples material under different orientations

The calculated results of mean crystallite size (Fig. 7, a) and atomic level strain (Fig. 7, b) study show that the crystallite size decreasing have influences on the microstrains and dislocation density and have correlation with mechanical properties (see Fig. 2) and their evolution during processing. The followed flat deformation and heat treatment at low temperatures, 170 °C and 350 °C, respectively [5] have large influence on the crystallites dimensions increase (Fig. 8, a) and atomic level strain decrease (Fig. 8, b).

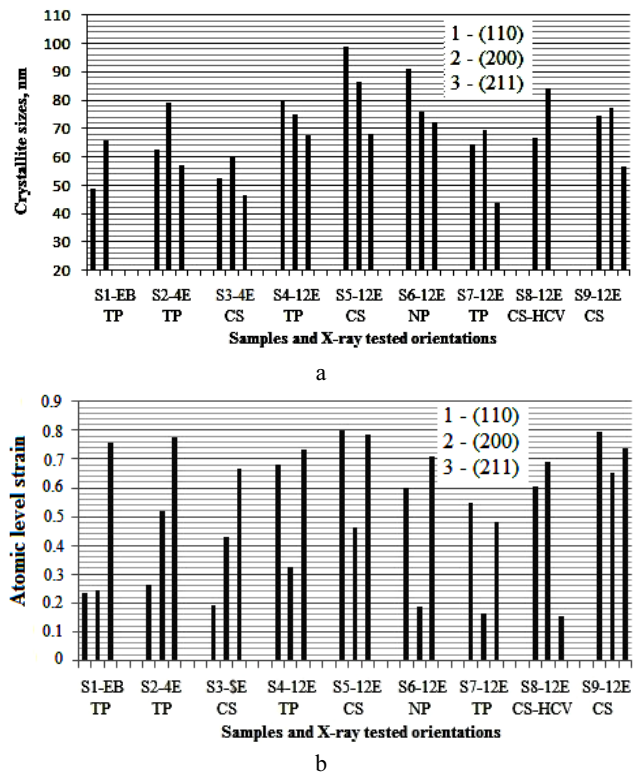


Fig. 7. Crystallite size (a) and corresponding atomic level strain (b) on atomic planes of (110), (200) and (211), respectively of pure Nb after ECAP. For samples S1 and S8 the crystallite sizes in (211) plane were 235 nm and 1995 nm, respectively

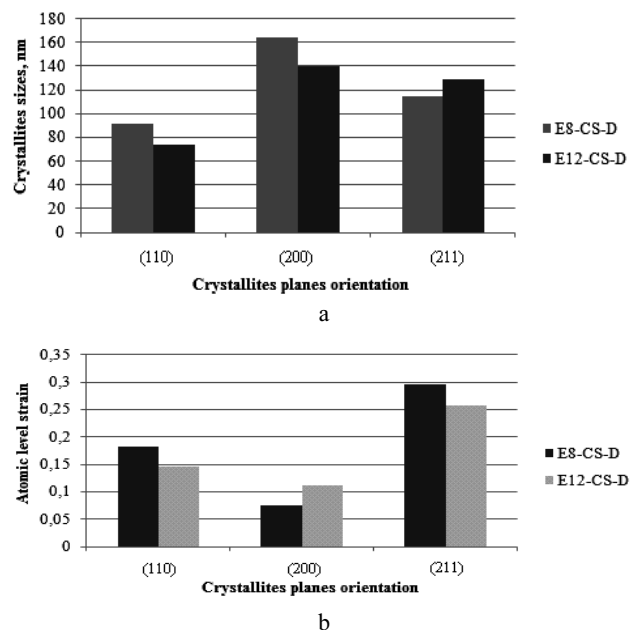


Fig. 8. Crystallites sizes (a) and atomic level strain (b) of Nb formed in samples of E8-CS-D and E12-CS-D after flat deformation and ageing at 170 °C and 350 °C, respectively

These changes were measured on flat deformed samples (after 8 and 12 passes of ECAP by B_c route) of pure Nb. Thus, these changes depend on ECAP passes number and planes orientation investigated. The crystallites dimensions studied by XRD and calculated according to [21] differed in different directions in the ECAP and HCV deformed samples as well in the different

crystal orientations directions and depended on ageing behavior, as well. The key factors of such changes in microstructure and properties of rare metal pure Nb at crystallite sizes decreased to nanometric dimensions (Fig. 7, a, and Fig. 8, a) and atomic level strain change (Fig. 7, b, and Fig. 8, b).

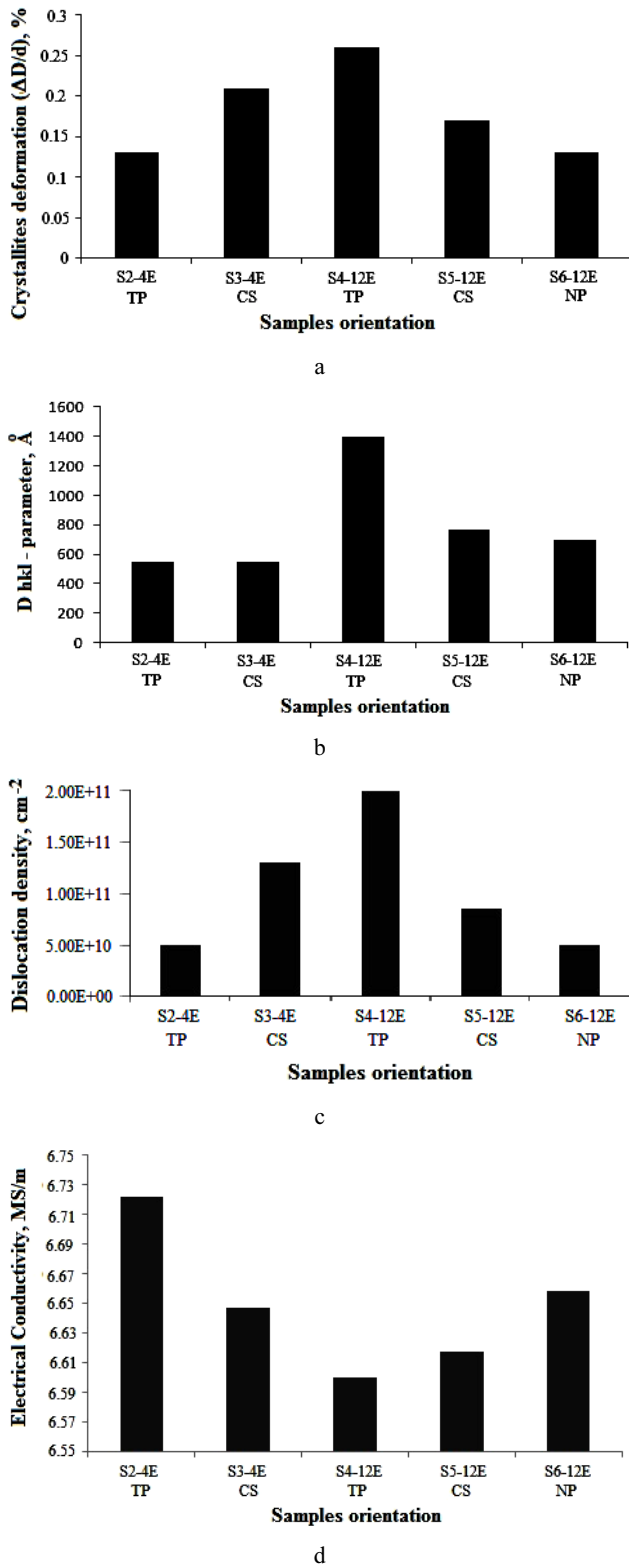


Fig. 9. Crystallites deformation (a), D hkl parameter (b) dislocation densities (c) and electrical conductivity (d) of pure Nb for different orientation of sample and ECAP passes number

The changes in the crystallites deformation degree (Fig. 9, a), D hkl-parameter (Fig. 9, b), dislocation density (Fig. 9, c) and corresponding electrical conductivity (Fig. 9, d) are as result of changes in the SPD processed pure Nb microstructure [23, 26].

It is well known [14] that electronic industries have a considerable demand for high electrical conductivity materials with high toughness and viscoelasticity properties.

For example, electrical conductivity of nanocrystalline niobium was decreased to 6.612 MS/m (Fig. 9, d) by dislocation density increase up to $2.0E+11$ cm⁻² (Fig. 9, c). The electrical conductivity was increased about 5 % during ageing at low temperatures as a result of corresponding crystallites dimensions and their deformation degree (Fig. 9, a), D hkl parameter (Fig. 9, b) and dislocation density (Fig. 9, c) decrease. These parameters are in opposite proportion with electrical conductivity. Therefore, for specimens with ECAP routes numbers from E3 to E8 pass the microhardness of Nb was increased in mean by 10 % during ageing treatment. The electrical conductivity of Nb decrease with increase of ECAP number and hardness parameters, and it increases with the decrease of dislocation density and relative microstrains (stresses) in atomic level at following HCV deformation. Results indicate, that the changes of mechanical and physical properties of Nb are related to low temperature heat treatment or ageing behavior and formed corresponding grain boundaries [21] in microstructure.

CONCLUSIONS

High purity Nb demonstrates relatively low strain hardening rate during SPD processing. After 8 passes of ECAP the Martens hardness was increased up to 3 times and after HCV deformation at five test series was increased up to 2.2 times.

The SPD processed Nb samples have mainly HAGB NC microstructure. The calculated mean crystallite size was 43.7 nm as minimal in crystallite plane of (211) of sample S7-12E-TP and maximal for the samples S1-EB-TP and S8-12E-CS-HCV with sizes of 235 nm and 1995 nm, respectively.

The atomic level strain in different samples and crystallite planes orientations are very differed and depend on calculation method also.

During flat deformation and ageing the atomic level strain and crystallite sizes were increased as compared to SPD processed condition. These changes depend on ECAP passes number and crystallite planes orientation.

The dislocation density varies from $5.0E+10$ cm⁻² to $2.0E+11$ cm⁻² and was maximal for pure niobium which has minimal electrical conductivity, maximal value of hkl-parameter and maximal microstresses or atomic level strain.

The correlation of atomic level strain to crystallite sizes depends on UFG microstructure sample orientation as well as on crystallite planes orientation, and needs investigation in the future.

Acknowledgments

The authors would like to acknowledge support from the Estonian Foundation Grant No SF140062s08.

Cooperation with co-authors mentioned in references is gratefully acknowledged as well.

REFERENCES

1. **Wei, Q., Ramesh, K. T., Kecskes, L. J., Mathaudhu, S. N., Hartwig, K. T.** Ultrafine and Nanostructured Refractory Metals Processed SPD: Microstructure and Mechanical Properties *Materials Science Forum* 579 2008: pp. 75–90.
2. **Kommel, L.** UFG Microstructure Processing by ECAP from Double Electron-beam Melted Rare Metal *Materials Science Forum* 584–586 2008: pp. 349–354.
3. **Kim, I.-H., Lee, J.-I., Choi, G.-S., Kim, J.-S.** Physical Properties Evaluation for High Purity Niobium and Tantalum Rare Metals *Advanced Materials Research* 26–28 2007: pp. 1059–1062.
4. **Sandim, H. R. Z., Bernardi, H. H., Verlinden, B., Raabe, D.** Equal Channel Angular Extrusion of Niobium Single Crystal *Materials Science and Engineering A* 467 2007: pp. 44–52.
5. **Kommel, L., Mikli, V., Traksmaa, R., Saarna, M., Pokatilov, A., Pikker, S., Kommel, I.** Influence of the SPD Processing Features on the Nanostructure and Properties of a Pure Niobium *Materials Science Forum* 667–669 2011: pp. 785–790.
6. **Grill, R., Gnadenberger, A.** Niobium as Mint Metal: Production-Properties-Processing *International Journal of Refractory Metals & Hard Materials* 24 2006: pp. 275–282.
<http://dx.doi.org/10.1016/j.ijrmhm.2005.10.008>
7. **Mathaudhu, S. N., Blum, S., Barber, R. E., Hartwig, K. T.** Severe Plastic Deformation of Bulk Nb for Nb₃Sn Superconductor *IEEE Transactions on Applied Superconductivity* 15 (2) 2005: pp. 3438–3441.
<http://dx.doi.org/10.1109/TASC.2005.849044>
8. **Langdon, T. G.** Processing by Severe Plastic Deformation: Historical Developments and Current Impact *Materials Science Forum* 667–669 2011: pp. 9–14.
9. **Valiev, R. Z., Langdon, T. G.** Principles of Equal-Channel Angular Pressing as a Processing Tool for Grain Refinement *Progress in Materials Science* 51 2006: pp.881–981.
10. **Gleiter, H.** Nanostructured Materials: Basic Concepts and Microstructure *Acta Materialia* 48 2000: pp. 1–29.
11. **Pande, C. S., Cooper, K. P.** Nanomechanics of Hall-Petch Relationship in Nanocrystalline Materials *Progress in Materials Science* 54 2009: pp. 689–706.
12. **Zhu, T., Li, J.** Ultra-strength materials *Progress in Materials Science* 55 2010: pp. 710–757.
<http://dx.doi.org/10.1016/j.pmatsci.2010.04.001>
13. **Lowe, T. C.** Status of Commercialization of Nanostructured Metals *Materials Science Forum* 667–669 2011: pp. 1145–1151.
14. **Kommel, L.** Properties Development of UFG Copper under Hard Cyclic Viscoplastic Deformation *Mater Letters* 64 2010: pp. 1580–1582.
<http://dx.doi.org/10.1016/j.matlet.2010.04.056>
15. **Kommel, L., Veinthal, R.** HCV Deformation - Method to Study the Viscoplastic Behavior of Nanocrystalline Metallic Materials *Review Advanced Materials Science* 10 2005: pp. 442–446.
16. **Kommel, L.** Metals Microstructure Improving under Hard Cyclic Viscoplastic Deformation *Materials Science Forum* 584–586 2008: pp. 361–366.
17. **Kommel, L., Hussainova, I., Volobueva, O.** Microstructure and Properties Development of Copper during Severe Plastic Deformation *Materials & Design* 28 2007: pp. 2121–2128.
18. **Aoki, M., Nguyen-Manh, D., Pettifor, D. G., Vitek, V.** Atom-based Bond-order Potentials for Modelling Mechanical Properties of Metals *Progress in Materials Science* 52 2007: pp. 154–195.
19. **Robin, A., Rosa, J. L.** Corrosion Behavior of Niobium, Tantalum and their Alloys in Hot Hydrochloric and Phosphoric Acid Solutions *International Journal of Refractory Metals & Hard Materials* 18 2000: pp. 13–21.
20. **Wurster, S., Pippin, R.** Nanostructured Metal under Irradiation *Scripta Materialia* 60 2009: pp. 1083–1087.
<http://dx.doi.org/10.1016/j.scriptamat.2009.01.011>
21. **Li, M., Xu, T.** Topological and Atomic Scale Characterization of Grain Boundary Networks in Polycrystalline and nanocrystalline materials *Progress in Materials Science* 56 2011: pp. 864–899.
<http://dx.doi.org/10.1016/j.pmatsci.2011.01.011>
22. **Egami, T.** Atomic Level Stresses *Progress in Materials Science* 56 2011: pp. 637–653.
<http://dx.doi.org/10.1016/j.pmatsci.2011.01.004>
23. **Wolf, D., Yamakov, V., Phillpot, S. R., Mukherjee, A., Gleiter, H.** Deformation of Nanocrystalline Materials by Molecular-Dynamics Simulation: Relationship to Experiments? *Acta Materialia* 53 2005: pp. 1–40.
<http://dx.doi.org/10.1016/j.actamat.2004.08.045>
24. **Vitek, V.** Atomic Level Computer Modeling of Crystal Defects with Emphasis on Dislocation: Past, Present and Future *Progress in Materials Science* 56 2011: pp. 577–585.
25. **Ikuhara, Y.** Nanowire Design by Dislocation Technology *Progress in Materials Science* 54 2009: pp. 770–791.
26. **Divinski, S. V., Reglitz, G., Rösner, H., Estrin, Y., Wilde, G.** Ultra-fast Diffusion Channels in Pure Ni Severely Deformed by Equal-Channel Angular Pressing *Acta Materialia* 59 2011: pp. 1974–1985.
<http://dx.doi.org/10.1016/j.actamat.2010.11.063>
27. **Lebensohn, R. A., Rollett, A. D., Suquet, R.** Fast Fourier Transform-based Modeling for the Determination of Micromechanical Fields in Polycrystals *JOM* 63 (3) 2011: pp. 13–18.
28. **Mathieu, J., Suwas, S., Eberhardt, A., Tóth, L., Moll, P.** A New Design for Equal Channel Angular Extrusion *Journal of Materials Processing Technology* 173 (1) 2006: pp. 29–33.
29. **Lamparter, P.** Information is available on: www.remax.ucoz.ru.
30. Information is available on: www.bruker-axs.com, TOPAS, Version.1.

Presented at the 20th International Baltic Conference
"Materials Engineering 2011"
(Kaunas, Lithuania, October 27–28, 2011)